



Secondary metabolites from *Etlingera rubroloba* rhizome: Profiling, isolation, structural elucidation, and evaluation of biological activities

Sahidin Sahidin^{1*}, Adryan Fristiohady¹, Muzuni Muzuni², Sitti Wirdhana Ahmad², Agung Wibawa Mahatva Yodha³, Arfan Arfan¹, Dzaky Aulia Rahman¹, Wahyuni Wahyuni¹, Irmanida Batubara⁴, Harlinda Kuspradini⁵, Femi Earnestly⁶, Andini Sundowo⁷

¹Faculty of Pharmacy, Halu Oleo University, Kendari, Indonesia.

²Department of Biology, Faculty of Mathematics and Natural Sciences, Universitas Halu Oleo, Kendari, Indonesia.

³Polytechnic of Bina Husada, Kendari, Indonesia.

⁴Department of Chemistry, Faculty of Mathematics and Natural Sciences, and Tropical Biopharmaca Research Center, IPB University, IPB Dramaga Campus, Bogor, Indonesia.

⁵Faculty of Forestry, Universitas Mulawarman, Samarinda, Indonesia.

⁶Faculty of Pharmacy, Muhammadiyah University of Sumatera Barat, Padang, Indonesia.

⁷Research Centre for Pharmaceutical Ingredient and Traditional Medicine, BRIN, KST BJ. Habibie, Tangerang Selatan, Indonesia.

ARTICLE HISTORY

Received on: 06/11/2025
Accepted on: 01/02/2026
Available Online: 05/03/2026

Key words:

Etlingera rubroloba,
secondary metabolites,
antioxidant, anti-
inflammatory, antidepressant.

ABSTRACT

Etlingera rubroloba is a traditional medicinal plant in Southeast Sulawesi, Indonesia. To date, no studies have been reported on the chemical and pharmacological aspects of *E. rubroloba* rhizomes. The total secondary metabolites of the methanol extract of *E. rubroloba* rhizome was analysed, by using the UPLC-High-Resolution Mass Spectrometry (HRMS) technique. It involves the isolation and structural elucidation of major compounds through chromatographic and spectroscopic methods, as well as an evaluation of the biological activities of the extracts and compounds, including antioxidant, anti-inflammatory, and antidepressant effects (the latter tested *in silico*). Six major compounds were identified for the first time from this species: Stigmasterol (ER1), Stigmast-4-en-6 β -ol-3-one (ER2), Yakuchinone A (ER3), 1-(3'-methoxy-4'-hydroxyphenyl)-7-(4''-hydroxyphenyl)-3-heptanone (ER4), 3,5-dimethoxy-4-acetoxy cinnamic alcohol (ER5), and *p*-Coumaric acid (ER6). The diarylheptanoids (ER3 and ER4) exhibited superior antioxidant activity, while the steroids (ER1 and ER2) demonstrated strong anti-inflammatory effects. Additionally, docking simulations suggested that ER1 and ER2 exhibited low binding energies towards monoamine oxidase, dopamine transporter, and serotonin transporter, indicating a possible relevance to neurotransmission pathways associated with depression. These findings highlight the chemical composition and pharmacological potential of *E. rubroloba* rhizomes, marking the first report of their antioxidant, anti-inflammatory, as well as their potential to interact with targets associated with depression, which represents a promising avenue for further confirmation through *in vitro* studies.

1. INTRODUCTION

In continuing our study on chemical and pharmaceutical aspects of *Etlingera* (Zingiberaceae) growing in the Wallace

area (Southeast Sulawesi province, Indonesia), *Etlingera rubroloba* rhizome is an interesting sample and to date, has not been reported yet. Previous research on this genus conducted by our group consisted of *E. calophrys* [1–3], *Etlingera elatior* rhizomes [4–7], *E. alba* rhizomes [8–11], *E. rubroloba* fruits [12,13], and *E. rubroloba* stems [14,15].

Fruits of *E. rubroloba* have potential immunomodulatory activity on macrophage phagocytosis and interleukin-12 levels in Bacillus Calmette–Guérin Vaccine (BCG)-stimulated

*Corresponding Author

Sahidin Sahidin, Faculty of Pharmacy, Halu Oleo University, Kendari, Indonesia. E-mail: sahidin02@uho.ac.id

Balb/C mice [12]. Two compounds, namely sinaphyl alcohol diacetate and ergosterol peroxide have been isolated from *E. rubroloba* fruits, which were potential as an immunomodulator agent [13]. Two compounds from *E. rubroloba* stems, sinapyl alcohol diacetate and stigmaterol, have potential as antihyperuricemia [14] and antioxidant and anti-inflammatory activities revealed by sinapyl alcohol acetate from this tissue [15]. Steroids and diarylheptanoids isolated from the rhizomes and stems of *E. calophrys* have been reported to exhibit antimicrobial and radical scavenging activities [2,3]. Another diarylheptanoids from *E. alba* rhizomes, called 1,7-diphenyl-6-heptene-3-one, can be developed as anti-metastatic for Tripel-Negative Breast Cancer [11]. The most popular of diarylheptanoids is curcumin, which is produced by plants such as rhizomes of *Curcuma longa* and *C. xanthorrhiza* (Zingiberaceae). This compound exhibits antidepressant potential through its potent antioxidant properties [16,17].

Based on a literature review of ScienceDirect and SpringerLink databases, no previous studies have reported the chemical or pharmacological aspects of *E. rubroloba* rhizomes. In particular, information on its chemical profile [using UPLC-High-Resolution Mass Spectrometry (HRMS)], isolation and structure elucidation, antioxidant and anti-inflammatory activities, and antidepressant potential is still lacking.

Therefore, this study aims to comprehensively investigate the chemical constituents and pharmacological properties of *E. rubroloba* rhizomes through integrated chemical analysis, biological assays, and *in silico* approaches. The novelty of this work lies in providing the first complete chemical and pharmacological characterization of *E. rubroloba* rhizomes, which not only expands the understanding of bioactive metabolites in the genus *Etlintera* but also supports its potential development as a natural source for novel antidepressant and anti-inflammatory agents.

2. MATERIAL AND METHODS

2.1 Plant material and preparation of the extract

Etlintera rubroloba rhizomes were collected from Punggaluku Village, Laeya District, South Konawe Regency, Southeast Sulawesi Province. The sample was identified and deposited at the BRIN Research Center for Biology, Cibinong, Indonesia, under the registration number 956/IPH.1.01/If.07/V/2019. The dried samples (1 kg) were macerated with methanol (Merck) for 72 hours and concentrated using a vacuum rotary evaporator (Stuart RE300, USA) to get 28 g of methanol extract.

2.2 UPLC-HRMS analysis of metabolites in the extract

HRMS is employed to identify chemical compounds, including metabolites and complex organic compounds in plant samples. The secondary metabolite content of the methanol extract was analyzed following previously reported methods [18]. The dried extract was reconstituted in MeOH-H₂O (1:1, v/v) to a final concentration of 1 mg/ml, centrifuged at 10,000 rpm for 10 minutes, and filtered through a 0.22 µm PTFE membrane prior to analysis. UPLC separation was performed using an ACQUITY BEH C18 column (2.1 × 100 mm, 1.7

µm) with a mobile phase consisting of water + 0.1% formic acid (A) and acetonitrile + 0.1% formic acid (B), applying a linear gradient from 5% to 95% B within 15 minutes at a flow rate of 0.3 ml/min. Injection volume was 5 µl, and the column temperature was maintained at 40°C. High-resolution Mass spectrometry was carried out on a Q-Exactive Orbitrap equipped with an Electrospray ionization source in positive and negative modes. Full scan spectra were acquired in the range m/z 100–1500 at 70,000 resolutions, followed by data-dependent MS/MS at 17,500 resolution using stepped collision energies of 20, 40, and 60 eV. The instrument was externally calibrated daily, and quantification was performed using six-point calibration curves from reference standards (quercetin) with caffeine (10 µg/ml) as an internal standard. Raw data were processed using Compound Discoverer 3.2 for peak alignment, deconvolution, and metabolite annotation based on accurate mass, isotopic distribution, and MS/MS spectra, further confirmed by comparison with mzCloud and authentic standards where available.

2.3 Isolation of secondary metabolite compounds

The methanol extract (20 g) was fractionated using vacuum liquid chromatography (VLC) with a 10 cm diameter column, silica gel GF254 as stationary phase (250 g), and a mobile phase consisting of an *n*-hexane:ethyl acetate mixture in varying ratios [8:2, 7:3, 5:5, 4:6, 2:8 (v/v)] and 100% methanol (200 ml each). This process yielded six fractions (1–6) weighing 4.24, 3.35, 0.36, 0.43, 2.56, and 8.22 g, respectively. The purification of fraction 3 by radial chromatography (RC) to get compound **ER1**, and in fraction 4, identified as compound **ER2**. Fraction 5 was further separated using RC with a silica gel GF254 stationary phase containing gypsum and a mobile phase of *n*-hexane:ethyl acetate [7:3 (v/v)] and 100% ethyl acetate, to get compounds **ER3** and **ER4**. Fraction 6 was also separated using RC with a silica gel GF254 adsorbent and eluent of *n*-hexane:ethyl acetate [5:5 (v/v)] and 100% ethylacetate. This resulted in six subfractions, with TLC analysis identifying a single spot in subfraction 3 as compound **ER5** and in subfraction 5 as compound **ER6**. Purity analysis for each compound was performed using TLC with a mobile phase of *n*-hexane:ethyl acetate [4:6 (v/v)].

2.4 Structure identification

The structures of the isolated compounds were determined using Nuclear Magnetic Resonance (NMR) spectroscopic techniques. The ¹H NMR and ¹³C NMR spectra were recorded on a Jeol JNM-ECZ500R/S1 NMR spectrometer (Japan) and a Bruker NMR spectrometer (USA). Molecular weight of each compounds were based on UPLC-HRMS data.

2.5 Biological activity

Antioxidant properties were evaluated using previously reported methods, focusing on the inhibition of 2,2-diphenyl-1-picrylhydrazyl (DPPH) radicals and 2,2-azino-bis-3-ethylbenzothiazoline-6-sulfonic acid (ABTS) radicals [19]. For the DPPH assay, a 0.1 mM DPPH solution in methanol was freshly prepared and adjusted to an absorbance of approximately 0.9–1.0 at 517 nm. Samples were prepared

as serial dilutions (1.56, 3.13, 6.25, 12.5, 25.0, 50.0, 100.0, and 200.0 $\mu\text{g/ml}$) and mixed with an equal volume of the DPPH solution in a 96-well microplate. The mixtures were incubated for 30 minutes at room temperature in the dark, and absorbance was measured at 517 nm. For the ABTS assay, the ABTS radical cation ($\text{ABTS}^{\bullet+}$) was generated by reacting 7 mM ABTS with 2.45 mM potassium persulfate for 16 hours in the dark at room temperature, and then diluted with ethanol to obtain an absorbance of 0.70 ± 0.02 at 734 nm. Aliquots of the samples at different concentrations were mixed with the $\text{ABTS}^{\bullet+}$ working solution, incubated for 6 min, and absorbance was measured at 734 nm. Trolox was used as the positive control, while reagent blanks and vehicle controls were included for correction. Replicates (n per group): each treatment group (sample, positive control, and vehicle control) was tested at eight concentrations, with $n = 3$ technical replicates per concentration in one run. Radical scavenging activity was expressed relative to the control, and IC_{50} values were determined from concentration response curves by linear regression.

The anti-inflammatory activity was assessed using the bovine serum albumin (BSA) protein denaturation inhibition method adapted from previous studies [20]. A stock solution of 5% (w/v) BSA was prepared in 0.05 M Tris-phosphate buffered saline (pH 6.5). Samples were dissolved in methanol (final solvent concentration $\leq 1\%$ v/v) and prepared as serial dilutions (1.56, 3.13, 6.25, 12.5, 25.0, 50.0, 100.0, and 200.0 $\mu\text{g/ml}$). In a 96-well microplate, BSA solution was mixed with the samples, incubated at 37°C for 15 minutes, then heated at 70°C for 5 minutes to induce protein denaturation, followed by cooling to room temperature. Turbidity was measured at 660 nm using a microplate reader. Methylprednisolone was used as the positive control; vehicle control and sample blanks (sample without BSA) were included for correction. Replicates (n per group): each treatment group (samples, positive control, and vehicle control) was tested at eight concentrations, with $n = 3$ technical replicates per concentration. Protein stabilization was expressed as the percentage of inhibition relative to the vehicle control. Potency was summarized as IC_{50} values obtained from concentration-response curves.

2.6 Statistical analysis

The collected data were presented as mean \pm SD and statistically analyzed by using IBM SPSS Statistics V26.0 software with one-way ANOVA analysis. The significance was exhibited at p -value < 0.05 .

2.7 In silico study

The three-dimensional structures of the target proteins in this study the Monoamine Oxidase (MOA) (PDB ID: 2BXS), dopamine transporter (DAT) (PDB ID: 4M48) [21], and serotonin transporter (SERT) (PDB ID: 516X) [22] were obtained from the Protein Data Bank. The molecular structures of the seven compounds identified in *E. rubroloba* rhizomes were retrieved from the PubChem database. Protein and ligand structures were prepared using AutoDockTools v1.5.6, following standard protocols [23]. Preparation of target proteins involved removing water molecules and bound ligands, protonation, and the addition of Kollman charges to ensure accurate electrostatic

properties [24]. To ensure docking reliability, known inhibitors from the co-crystal structures were employed as positive controls: clorgyline for MAO, nortriptyline for DAT, and paroxetine for SERT. Docking simulations were conducted using AutoDock Vina [25] with an exhaustiveness parameter set to 64 to ensure thorough conformational sampling, generating nine binding poses for each ligand. The top-ranked pose based on binding affinity was selected for interaction analysis using Discovery Studio Visualizer.

Docking grids were defined to encompass the active site residues identified from the co-crystallized ligands, with the following parameters: MAO (grid center: $x = 10.192$, $y = 125.199$, $z = 51.599$; grid size: $20 \times 20 \times 20 \text{ \AA}$), DAT (grid center: $x = -39.808$, $y = -1.239$, $z = 55.308$; grid size: $25 \times 25 \times 25 \text{ \AA}$), and SERT (grid center: $x = -31.847$, $y = -20.608$, $z = 2.120$; grid size: $25 \times 25 \times 25 \text{ \AA}$). The docking protocol was validated through redocking of the co-crystallized ligands into their respective binding sites. The Root Mean Square Deviation values between the docked and crystallographic poses were 1.220 \AA for clorgyline with MAO, 0.578 \AA , or nortriptyline with DAT, and 0.723 \AA for paroxetine with SERT, all below the 2 \AA threshold, indicating accurate reproduction of experimental binding modes (Fig. 5).

3. RESULTS AND DISCUSSION

The extraction results revealed that the yield of *E. rubroloba* rhizome methanol extract was 2.8%. The chromatogram from the chemical compound analysis of the extract (Fig. 1), based on UPLC-HRMS data within the retention time (RT) range of 0–25 minutes, displayed distinct peaks.

The analysis revealed 48 major compounds present in the rhizomes of *E. rubroloba*. The chemical content plays a significant role in contributing to the biological properties of the species. By understanding the chemical composition, the study of metabolite compounds with potential biological activity can be carried out, facilitating the isolation of these compounds. Six isolated compounds from *E. rubroloba* rhizome consist of ER1, ER2, ER3, ER4, ER5, and ER6, displayed at (Fig. 2), with ^1H NMR and ^{13}C NMR spectra could be summarized as follows.

ER1. White powder; $\text{C}_{29}\text{H}_{48}\text{O}$. ^1H NMR (CDCl_3 , 500.159 MHz, chemical shift δ in ppm, coupling constant J in Hz) 5.34 (1H, *m*, H-6), 5.14 (1H, *dd*, 8.5; 15.5, H-22), 5.00 (1H, *dd*, 8.5; 15.5, H-23), 3.34 (1H, *m*, H-3), 1.00 (3H, *s*, H-18), 0.91 (3H, *d*, 7, H-21), 0.83 (3H, *m*, H-29), 0.82 (3H, *m*, H-29), 0.80 (3H, *m*, H-29), 0.67 (3H, *s*, H-19). ^{13}C NMR (CDCl_3 , 125.765 MHz, chemical shift δ in ppm) 140.9 (C-5), 138.4 (C-23), 129.4 (C-22), 121.8 (C-6), 71.9 (C-3), 56.9 (C-14), 56.1 (C-17), 50.2 (C-9), 45.9 (C-24), 42.4 (C-4), 42.4 (C-13), 40.6 (C-20), 39.9 (C-12), 37.4 (C-1), 36.7 (C-10), 32.0 (C-2), 32.0 (C-7), 31.7 (C-8), 29.3 (C-27), 28.4 (C-16), 26.2 (C-28), 24.4 (C-15), 23.2 (C-21), 21.2 (C-11), 20.0 (C-26), 19.5 (C-27), 18.9 (C-19), 12.1 (C-18) and 12.0 (C-29).

ER2. White powder; $\text{C}_{29}\text{H}_{48}\text{O}_2$. ^1H NMR ($(\text{CD}_3)_2\text{CO}$, 700.302 MHz, chemical shift δ in ppm, coupling constant J in Hz) 5.69 (1H, *s*, H-4), 4.30 (1H, *d*, 8.6 Hz, H-6), 1.41 (3H, *s*, H-19), 0.98 (3H, *d*, 6.5 Hz, H-21), 0.88 (3H, *d*, 7.3

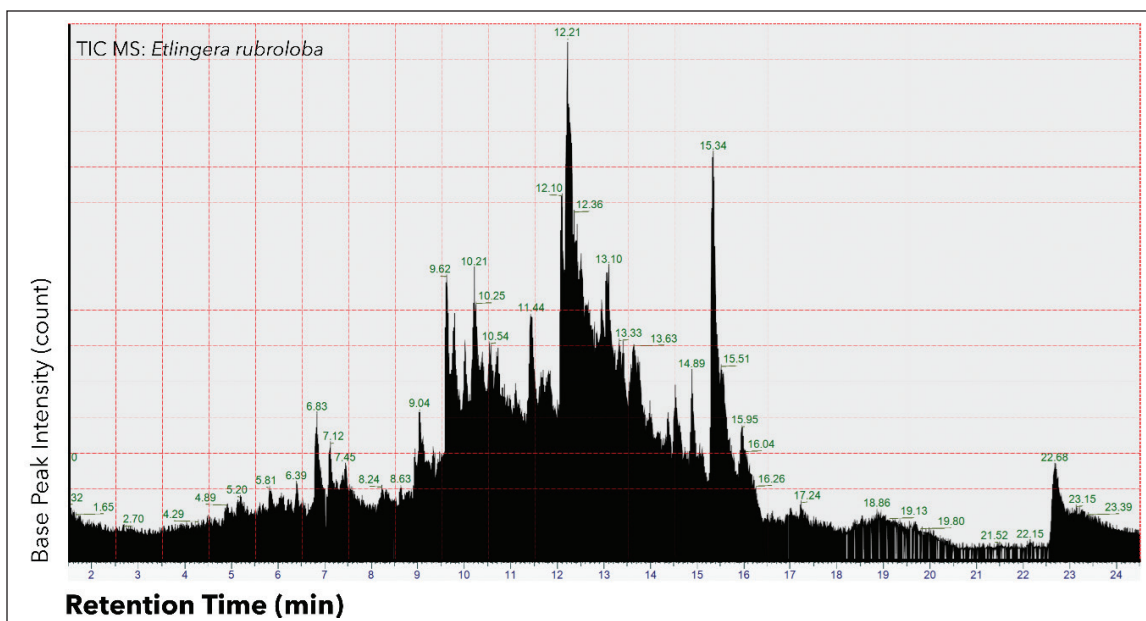


Figure 1. UPLC-MS chromatogram of the methanol extracts of the *E. rubroloba* rhizome.

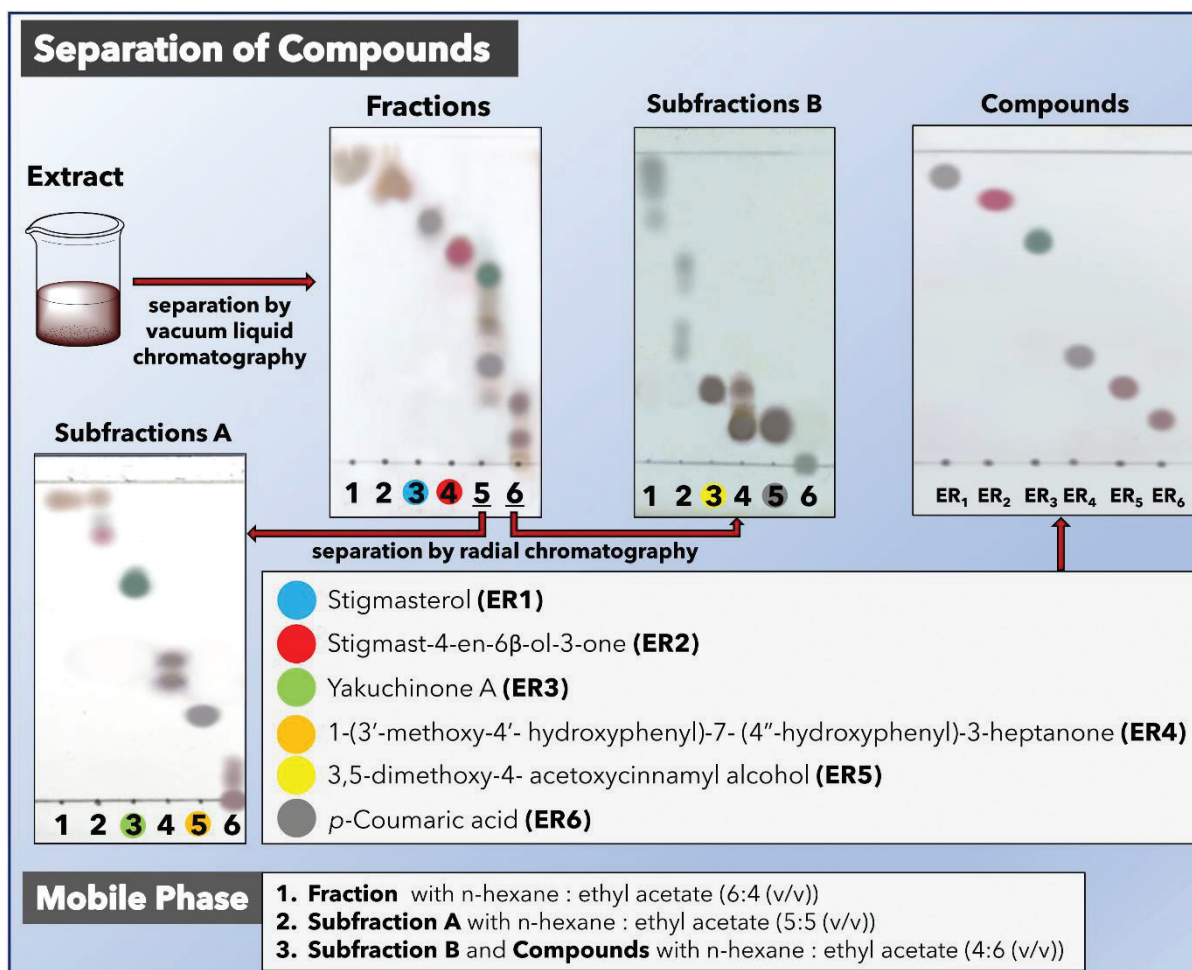


Figure 2. Isolation of secondary metabolite compounds from *E. rubroloba* rhizomes.

Table 1. Secondary metabolites in the methanol extracts of *E. rubroloba* rhizome.

No	RT (min)	Calc. MW	Formula	Compound ame	Area [BPI]	Delta mass (ppm)
1	1.147	226.0839	C ₁₁ H ₁₄ O ₅	3,4,5-Trimethoxyphenyl acetate	62,125,033.5	-0.94
2	5.165	164.0473	C₉H₈O₃	p-Coumaric acid	212,270,699.9	-0.46
3	6.042	330.1461	C ₁₉ H ₂₂ O ₅	1,7-bis(3,4-dihydroxyphenyl) heptan-3-one	82,656,462.9	-1.99
4	6.844	185.2141	C ₁₂ H ₂₇ N	Tributylamine	613,921,790.6	-1.61
5	7.581	252.0995	C₁₃H₁₆O₅	3,5-dimethoxy-4- acetoxycinnamyl alcohol	841,400,105.1	-1.25
6	8.700	328.1669	C ₂₀ H ₂₄ O ₄	Croctetin	143,115,946.1	-1.65
7	9.044	148.0522	C ₉ H ₈ O ₂	Cinnamic acid	72,186,893.4	-1.54
8	9.046	372.1564	C ₂₁ H ₂₄ O ₆	1-(2,4-Dihydroxy-5-methoxyphenyl)-7-(3-methoxyphenyl)-3,5-heptanedione	473,628,904.9	-2.42
9	9.138	316.0577	C ₁₆ H ₁₂ O ₇	2-(3,4-dihydroxyphenyl)-3,5,7-trihydroxy-6-methyl-4H-chromen-4-one	117,59,9157.5	-1.92
10	9.754	317.2921	C ₁₈ H ₃₉ NO ₃	2-Amino-1,3,4-octadecanetriol	593,185,760.9	-2.72
11	9.780	296.1406	C ₁₉ H ₂₀ O ₃	(4E)-1,7-Bis(4-hydroxyphenyl)-4-hepten-3-one	82,488,185.6	-2.14
12	9.783	433.2093	C ₂₃ H ₃₁ NO ₇	Mycophenolate mofetil	255,008,161.3	-1.72
13	9.785	356.1616	C ₂₁ H ₂₄ O ₅	Odoratisol A	399,075,683.8	-2.32
14	10.017	144.0573	C ₁₀ H ₈ O	1-Naphthol	305,196,215.1	-1.69
15	10.245	328.1667	C₂₀H₂₄O₄	1-(3'-methoxy-4'- hydroxyphenyl)-7-(4"-hydroxyphenyl)-3-heptanone	568,317,610.2	-2.26
16	10.277	234.0889	C ₁₃ H ₁₄ O ₄	7-Hydroxy-2-(2-hydroxypropyl)-5-methyl-4H-chromen-4-one	60,917,917.5	-1.39
17	10.479	314.0787	C ₁₇ H ₁₄ O ₆	Myricetin	68,662,223.3	-1.2
18	10.706	304.2034	C ₁₉ H ₂₈ O ₃	16-hydroxytestosterone	77,014,298.3	-1.39
19	10.778	266.1879	C ₁₆ H ₂₆ O ₃	Tetranor 12-HETE	80,630,083.81	-1.12
20	11.201	250.1931	C ₁₆ H ₂₆ O ₂	4-tert-Octylphenol monoethoxylate	119,562,048.3	-0.73
21	11.204	146.0367	C ₉ H ₆ O ₂	Coumarin	96,909,389.2	-0.65
22	11.413	296.1772	C ₂₀ H ₂₄ O ₂	Ethinylestradiol	200,143,430.3	-1.44
23	11.442	134.1094	C ₁₀ H ₁₄	p-Cymene	204,277,353.9	-0.99
24	12.092	312.172	C₂₀H₂₄O₃	Yakuchinone A	701,945,554.6	-1.85
25	12.232	148.1251	C ₁₁ H ₁₆	n-Amylbenzene	76,486,075.4	-1.03
26	12.237	190.1717	C ₁₄ H ₂₂	1,3-Di-tert-butylbenzene	1,948,646,557.0	-2.24
27	12.431	278.2243	C ₁₈ H ₃₀ O ₂	α-Eleostearic acid	71,276,217.3	-1.15
28	12.512	288.2084	C ₁₉ H ₂₈ O ₂	Testosterone	64,4105,044.4	-1.83
29	12.514	306.2188	C ₁₉ H ₃₀ O ₃	11-Hydroxyetiocolanolone	170,356,852.4	-2.18
30	12.557	288.2449	C ₂₀ H ₃₂ O	Ethylestrenol	209,789,603.3	-1.48
31	12.667	314.224	C ₂₁ H ₃₀ O ₂	Progesterone	110,511,558.1	-1.99
32	12.668	350.2449	C ₂₁ H ₃₄ O ₄	Tetrahydro-11-deoxycortisol	257,115,037.3	-2.2
33	12.822	294.219	C ₁₈ H ₃₀ O ₃	(10E,12Z)-9-oxooctadeca-10,12-dienoic acid	121,046,943.7	-1.61
34	13.335	162.1406	C ₁₂ H ₁₈	Hexylbenzene	57,544,975.2	-1.29
35	13.645	348.2294	C ₂₁ H ₃₂ O ₄	3,17,21-Trihydroxypregn-2-en-1-one	69,4250,398.5	-2.04
36	13.739	282.1983	C ₂₀ H ₂₆ O	Dehydroretinaldehyde	109,425,595.2	-0.38
37	14.000	354.2763	C ₂₁ H ₃₈ O ₄	1-Linoleoyl glycerol	58,923,475.5	-1.97
38	14.615	402.3126	C ₂₆ H ₄₂ O ₃	4-Allyl-2-methoxyphenyl palmitate	61,037,734.5	-1.88
39	14.623	264.2452	C ₁₈ H ₃₂ O	2-[(5Z)-5-tetradecenyl] cyclobutanone	373,833,551.1	-0.57
40	14.897	162.1406	C ₁₂ H ₁₈	Hexylbenzene	153,492,893.6	-1.29
41	15.341	284.2134	C ₂₀ H ₂₈ O	(9cis)-Retinal	5,873,347,815.0	-2.12
42	15.443	272.2499	C ₂₀ H ₃₂	syn-labda-8(17),12E,14-triene	89,658,451.06	-1.97

Continued

No	RT (min)	Calc. MW	Formula	Compound ame	Area [BPI]	Delta mass (ppm)
43	15.964	418.3075	C ₂₆ H ₄₂ O ₄	Maxacalcitol	369,254,566.5	-1.85
44	16.243	511.4957	C ₃₂ H ₆₅ NO ₃	C14-Dihydroceramide	191,350,557.3	-1.43
45	16.929	428.3647	C₂₉H₄₈O₂	Stigmast-4-en-6β-ol-3-one	178,739,474.9	-1.76
46	17.032	539.5272	C ₃₄ H ₆₉ NO ₃	C16-Dihydroceramide	145,546,559.9	-0.99
47	18.371	424.3337	C ₂₉ H ₄₄ O ₂	4,4'-Methylenebis	74,563,926.84	-1.1
48	18.904	412.3697	C₂₉H₄₈O	Stigmasterol	382,572,989.4	-1.89

Hz, H-29), 0.87 (3H, d, 6.9 Hz, H-26), 0.85 (3H, d, 6.9 Hz, H-27) and 0.79 (3H, s, H-18); ¹³C NMR ((CD₃)₂CO, 176.108 MHz, chemical shift δ in ppm) 200.7 (C-3), 168.6 (C-5), 125.3 (C-4), 72.2 (C-6), 56.0 (C-17), 55.8 (C-14), 53.8 (C-9), 45.8 (C-24), 42.9 (C-13), 39.8 (C-12), 39.6 (C-7), 37.9 (C-10), 37.1 (C-1), 36.0 (C-20), 33.9 (C-2), 33.7 (C-22), 29.7 (C-8), 29.1 (C-25), 28.0 (C-16), 25.8 (C-23), 23.9 (C-15), 22.8 (C-28), 20.8 (C-11), 19.2 (C-26), 18.7 (C-19), 18.4 (C-27), 18.2 (C-21), 11.4 (C-18) and 11.3 (C-29).

ER3. Yellow oil; C₂₀H₂₄O₃. ¹H NMR (CDCl₃, 500.159 MHz, chemical shift δ in ppm, coupling constant J in Hz) 7.26 (2H, m, H-3"/H-5"), 7.17 (1H, m, H-4"), 7.14 (2H, m, H-2"/H-6"), 6.81 (1H, d, 8.0, H-5'), 6.67 (1H, d, 1.5, H-2'), 6.64 (1H, dd, 2.0 & 8.0, H-6'), 3.84 (3H, s, H-7'), 2.81 (2H, t, 7.5, H-1), 2.67 (2H, t, 7.5, H-2), 2.38 (2H, t, 7.0, H-4), 2.59 (2H, t, 7.0, H-7) and 1.59 (4H, m, H-5/H-6); ¹³C NMR (CDCl₃, 125.765 MHz, chemical shift δ in ppm) 210.3 (C-3), 146.4 (C-3'), 143.9 (C-4'), 142.2 (C-1"), 133.1 (C-1'), 128.4 (C-3"/C-5"), 128.3 (C-2"/C-6"), 125.8 (C-4"), 120.8 (C-6'), 114.4 (C-5'), 111.1 (C-2'), 55.9 (C-7'), 44.7 (C-2), 42.9 (C-4), 35.8 (C-7), 31.0 (C-6), 29.6 (C-1) and 23.4 (C-5).

ER4. Yellow oil; C₂₀H₂₄O₄. ¹H NMR (CDCl₃, 500.159 MHz, chemical shift δ in ppm, coupling constant J in Hz) 7.00 (2H, m, H-2", H-6"), 6.82 (1H, d, 8.0, H-5'), 6.74 (2H, m, H-3", H-5"), 6.67 (1H, d, 2.0, H-2'), 6.65 (1H, dd, 2.0 & 8.0, H-6'), 3.85 (3H, s, H-7'), 2.81 (2H, t, 7.5, H-1), 2.67 (2H, t, 8, H-2), 2.52 (2H, t, 7.5, H-7), 2.38 (2H, t, 7.0, H-4), 1.59 (2H, m, H-5) and 1.54 (2H, m, H-6); ¹³C NMR (CDCl₃, 125.765 MHz, chemical shift δ in ppm) 210.6 (C-3), 153.8 (C-4"), 146.5 (C-3'), 144.0 (C-4'), 134.4 (C-1"), 133.2 (C-1'), 129.5 (C-2"/C-6"), 120.9 (C-6'), 115.3 (C-3"/C-5"), 114.5 (C-5'), 111.2 (C-2'), 56.0 (C-7'), 44.8 (C-2), 43.1 (C-4), 34.9 (C-7), 31.3 (C-6), 29.7 (C-1) and 23.5 (C-5).

ER5. White oil; C₁₃H₁₆O₅. ¹H NMR (CDCl₃, 500.159 MHz, chemical shift δ in ppm, coupling constant J in Hz) 6.61 (2H, s, H-2/H-6), 6.54 (1H, d, 15.5, H-7), 6.30 (1H, dt, 15.5 & 6.0, H-8), 4.31 (2H, d, 6.0, H-9), 3.81 (6H, s, H-10, H-13), 2.32 (3H, s, H-12); ¹³C NMR (CDCl₃, 125.765 MHz, chemical shift δ in ppm) 168.9 (C-11), 152.2 (C-3/C-5), 135.2 (C-1), 130.9 (C-7), 129.0 (C-8), 128.5 (C-4), 103.1 (C-2, C-6), 63.5 (C-9), 56.1 (C-10/C-13) and 20.5 (C-12).

ER6. White powder; C₉H₈O₃. ¹H NMR ((CD₃)₂CO, 400.172 MHz, chemical shift δ in ppm, coupling constant J in Hz) 8.97 (1H, s), 7.63 (1H, d, 15.6, H-7), 7.57 (2H, d, 8.8 Hz, H-2/H-6), 6.91 (2H, d, 8.8 Hz, H-3/H-5) and 6.34 (1H, d,

15.6, H-8). ¹³C NMR ((CD₃)₂CO, 400.172 MHz, chemical shift δ in ppm) 167.2 (C-9), 159.6 (C-4), 144.6 (C-7), 130.0 (C-2/C-6), 126.1 (C-1), 115.7 (C3/C-5), and 114.8 (C-8).

Forty-eight major compounds were identified by UPLC-HRMS from rhizomes of *E. rubroloba*, six of 48 compounds were successfully isolated using chromatographic techniques, and their structures were determined through NMR data interpretation (Table 2) and molecular weight of UPLC-HRMS data (Table 1).

ER1 and ER2 are identified as steroids. It is supported by the carbon NMR spectra (Table 2), specifically identifiable due to the presence of 29 carbon atoms. The carbonyl carbon (C=O) signal appears in a more downfield region (around 200 ppm), while the methyl carbon at positions C18, C19, C26, C27, and C29 appears in the δ ≈ 10–20 ppm region. The carbon at δ ≈ 70 ppm, namely C3 (ER1) and C6 (ER2), experiences deshielding due to the presence of oxygen atom substituents, which significantly shifts the carbon chemical shift value to a higher ppm. This shift correlates directly with the chemical shift observed in proton NMR. Through a literature search comparing NMR spectroscopic data, it can be concluded that compound ER1 is Stigmasterol [3], while compound ER2 is Stigmast-4-en-6-ol-3-one [26,27] (Table 2), and with molecular weight is relevant to compounds 25 and 48, respectively, in Table 1.

Diarylheptanoids are compounds consisting of two aromatic rings connected by a seven-carbon chain (C6-C7-C6). The same way as the structure elucidation of steroids, ER3 is Yakuchinone A [3] and ER4 is 1-(3'-methoxy-4'-hydroxyphenyl)-7-(4"-hydroxyphenyl)-3-heptanone [26,27] with a molecular weight of relevant to compounds 24 and 15 in Table 1, respectively. Through a literature search comparing NMR spectroscopic data, it can be observed that compound ER5 is 3,5-dimethoxy-4-acetoxycinnamyl alcohol [11] and compound ER6 is p-Coumaric acid with molecular weight is relevant to compounds 5 and 2 in Table 1, respectively. The molecular structure of the isolated compounds is presented in Figure 3.

Biological activities of methanol extract and six compounds towards DPPH, ABTS, and BSA displayed in (Fig. 4), and in-silico study as an antidepressant potential of six compounds were shown in Table 3.

Methanol extract of *E. rubroloba* (ER) rhizome and some isolated compounds demonstrated strong antioxidant and anti-inflammatory activities. The statistical analysis showed that there were significant differences between several treatment groups and the positive control (*p* < 0.05).

Table 2. ¹H and ¹³C NMR data of compounds ER1 and ER2 compared with data from literature (ER1* and ER2*)

No	ER1		ER1*		ER2		ER2*	
	δ_c	δ_H ($\Sigma H, m, J = Hz$)	δ_c	δ_H ($\Sigma H, m, J = Hz$)	δ_c	δ_H ($\Sigma H, m, J = Hz$)	δ_c	δ_H ($\Sigma H, m, J = Hz$)
1	37.4		37.6		37.1		37.2	
2	32.0		32.1		33.9		33.9	
3	71.9	3.51 (1H, m)	72.1	3.51 (1H, tdd, 4.5; 4.4; 3.8)	200.7		200.7	
4	42.4		42.4		125.3	5.69 (1H, s)	125.4	5.82 (1H, s)
5	140.9		141.1		168.6		168.6	
6	121.8	5.34 (1H, m)	121.8	5.31 (1H, t, 6.1)	72.2	4.30 (1H, d, 8.6)	72.3	4.34 (1H, m)
7	32.0	-	31.8	-	39.6	-	39.6	-
8	31.7	-	31.8	-	29.7	-	29.7	-
9	50.2	-	50.2	-	53.8	-	53.9	-
10	36.7	-	36.6	-	37.9	-	37.9	-
11	21.2	-	21.5	-	20.8	-	20.8	-
12	39.9	-	39.9	-	39.8	-	39.7	-
13	42.4	-	42.4	-	42.9	-	42.9	-
14	56.9	-	56.8	-	55.8	-	55.9	-
15	24.4	-	24.4	-	23.9	-	24.0	-
16	28.4	-	29.3	-	28.0	-	28.1	-
17	56.1	-	56.2	-	56.0	-	56.1	-
18	12.1	1.00 (3H, s)	12.2	1.03 (3H, s)	11.4	0.79 (3H, s)	11.5	0.75 (3H, s)
19	18.9	0.67 (3H, s)	18.9	0.71 (3H, s)	18.7	1.41 (3H, s)	18.8	1.38 (3H, s)
20	40.6	-	40.6	-	36.0	-	36.0	-
21	23.2	0.91 (3H, d, 7)	21.7	0.91 (3H, d, 6.2)	18.2	0.98 (3H, d, 6.5)	18.3	0.93 (3H, d, 6.5)
22	129.4	5.14 (1H, dd, 8.5; 15.5)	129.6	5.14 (1H, m)	33.7	-	33.8	-
23	138.4	5.00 (1H, dd, 8.5; 15.5)	138.7	4.98 (1H, m)	25.8	-	25.9	-
24	45.9	-	46.1	-	45.8	-	45.8	-
25	29.3	-	29.6	-	29.1	-	29.1	-
26	20.0	0.82 (3H, m)	20.2	0.82 (3H, d, 6.6)	19.2	0.87 (3H, d, 6.9)	19.2	0.84 (3H, d, 6.1)
27	19.5	0.80 (3H, m)	19.8	0.80 (3H, d, 6.6)	18.4	0.85 (3H, d, 6.9)	18.5	0.82 (3H, d, 6.1)
28	26.2	-	25.4	-	22.8	-	22.9	-
29	12.0	0.83 (3H, m)	12.1	0.83 (3H, t, 7.1)	11.3	0.88 (3H, d, 7.3)	11.4	0.85 (3H, t, 6.7)

ER1*3 ER2*26,2727.

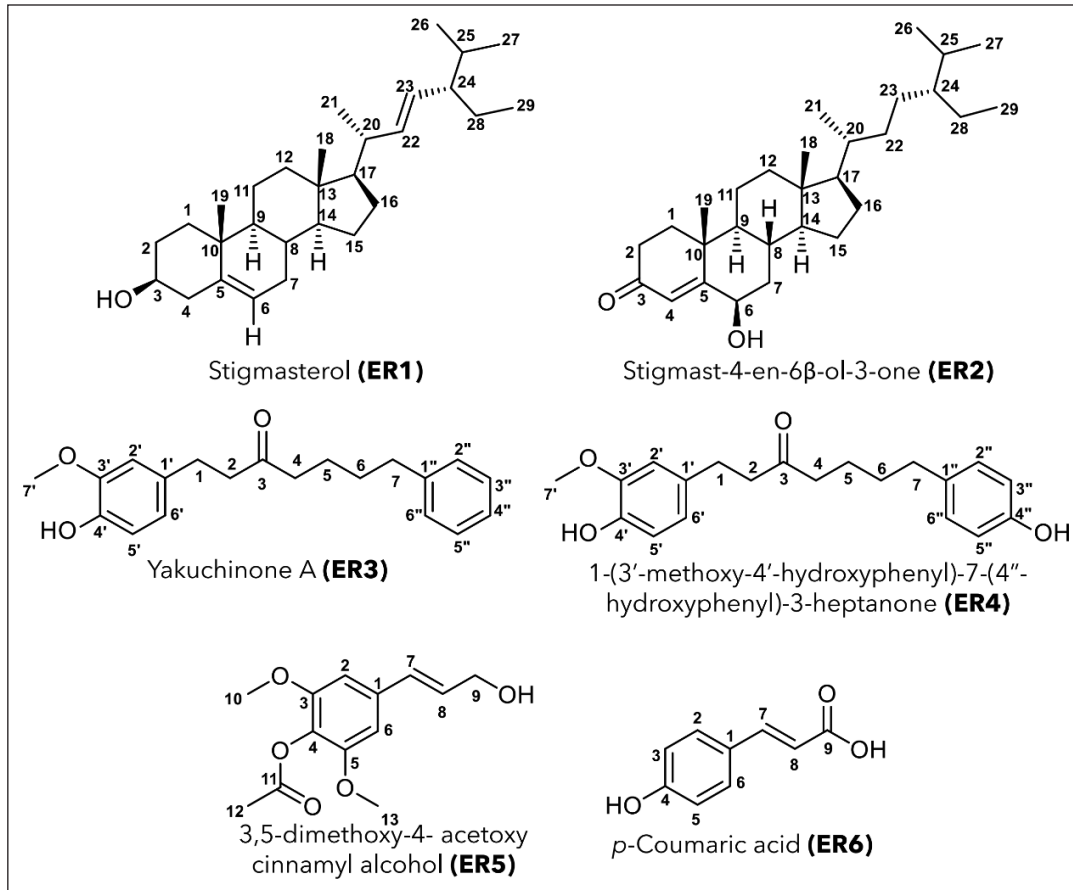


Figure 3. Structure of isolated compounds from *E. rubroloba* rhizome.

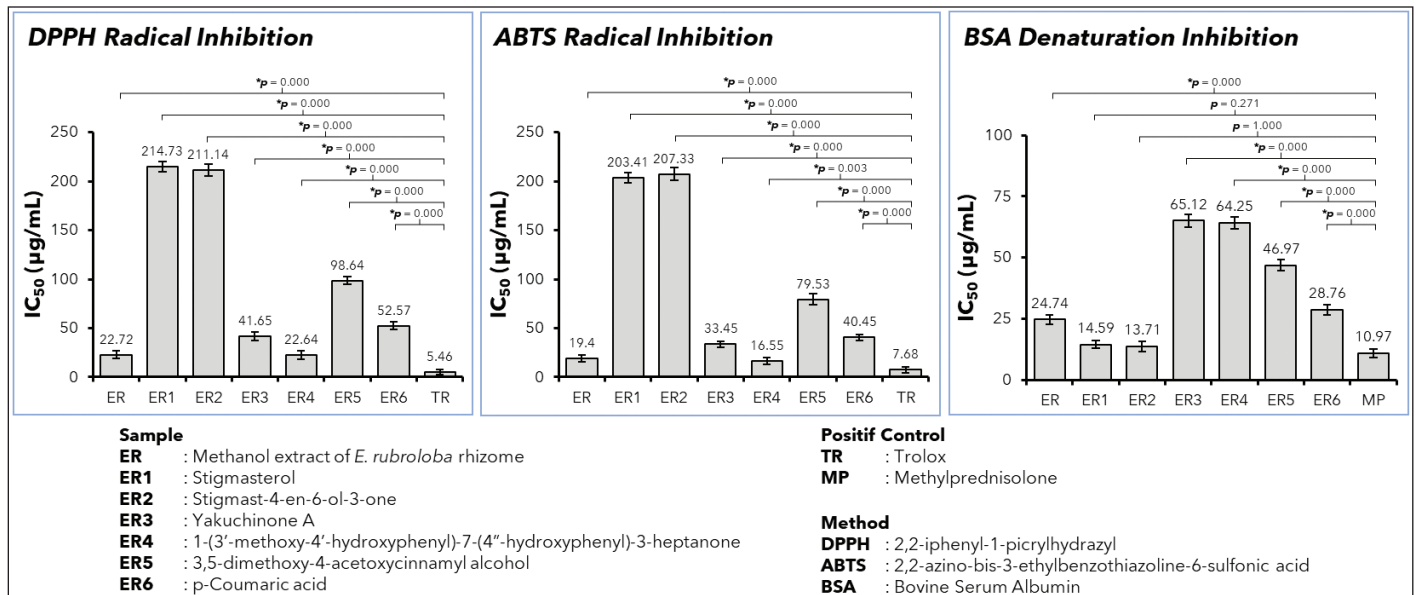


Figure 4. Biological activity of *E. rubroloba* methanol extract and isolated secondary metabolite compounds. Data is presented as mean \pm SD (n=3). * indicates the significancy compared to positif control.

This indicates that the activity exhibited by the test samples was significantly lower than that of the positive control. Conversely, in certain treatment groups, the difference with

the positive control was not significant ($p > 0.05$), suggesting that the activity produced was comparable to the effectiveness of the positive control.

In the DPPH and ABTS radical scavenging assays (Fig. 4), most of the test samples exhibited $p < 0.05$ when compared with the positive control, indicating significant differences. This confirms that although the samples possessed activity, the potential they demonstrated was still lower than that of the standard control. Meanwhile, in the BSA denaturation inhibition assay, some test groups showed $p > 0.05$, indicating that their biological activity was comparable to the positive control.

Two steroid compounds, stigmasterol (ER1) and Stigmast-4-en-6 β -ol-3-one (ER2), showed no significant difference compared to methylprednisolone as the control. Overall, the statistical results reinforced the validity of the finding that the positive control consistently provided higher effects. However, samples that showed $p > 0.05$ compared to the positive control deserve particular attention, as they potentially possess effectiveness equivalent to the standard comparator.

This synergistic action of antioxidant and anti-inflammatory properties presents an opportunity to explore their potential as antidepressant agents. The link between antioxidants, anti-inflammation, and antidepressants lies in the capacity of these compounds to address two key components of depression: oxidative stress and inflammation. By reducing

oxidative damage and inflammation, compounds with antioxidant and anti-inflammatory properties can improve neurotransmitter balance and alleviate depressive symptoms [28].

Docking results of six compounds against target proteins MAO, DAT, and SERT to predict their antidepressant activity revealed that stigmast-4-en-6 β -ol-3-one and stigmasterol were the most notable compared to other compounds (Table 3). Stigmast-4-en-6 β -ol-3-one and stigmasterol demonstrated the highest potential as antidepressants, based on their binding affinities, particularly against MAO, with binding energies of -11.9 and -11.5 kcal/mol, respectively. In general, all compounds from the *E. rubroloba* rhizome exhibited promising potential against the MAO target compared to Clorgyline. Notably, stigmast-4-en-6 β -ol-3-one and stigmasterol showed stronger affinities than Nortriptyline and Paroxetine against the DAT and SERT targets.

In targeting MAO, stigmast-4-en-6 β -ol-3-one exhibited a binding energy of -11.9 kcal/mol, which is lower than that of stigmasterol (-11.5 kcal/mol) and the positive control clorgyline (-6.6 kcal/mol). Stigmast-4-en-6 β -ol-3-one formed a hydrogen bond with Cys406 and demonstrated hydrophobic interactions with key residues such as Phe352, Val210, Cys323, Leu337, Ile335, Phe208, Tyr69, Tyr407, and Tyr444 (Fig. 6A), indicating strong binding at the MAO active site [22]. This suggests that stigmast-4-en-6 β -ol-3-one may serve as a more efficient inhibitor, potentially contributing significantly to the inhibition of this enzyme. Although stigmasterol did not form hydrogen bonds, it still displayed stable hydrophobic interactions with residues similar to those of stigmast-4-en-6 β -ol-3-one, indicating sufficient binding stability (Fig. 6B).

MAO is an enzyme responsible for the oxidative deamination of neurotransmitters such as serotonin, dopamine, and norepinephrine. There are two major isoforms: MAO-A and MAO-B. Inhibition of MAO, particularly MAO-A, increases neurotransmitter concentrations at synapses by reducing their degradation, which is important in mood regulation [29]. In the context of molecular docking, both stigmast-4-en-6 β -ol-3-one and stigmasterol exhibited lower binding energies than the standard inhibitor clorgyline, indicating their potential to inhibit MAO activity. Inhibition of this enzyme would elevate serotonin, dopamine, and norepinephrine levels in the brain, which are directly linked to improved mood and reduced depression symptoms.

Table 3. Binding energies from the docking results of six compounds from the *E. rubroloba* against the target proteins MAO, DAT, and SERT.

No	Compounds	Binding Energies (kcal/mol)		
		MAO	DAT	SERT
1	Stigmast-4-en-6 β -ol-3-one	-11.9	-10.7	-10.5
2	Stigmasterol	-11.5	-10.7	-10.1
3	1-(3'-methoxy-4'-hydroxyphenyl)-7-(4''-hydroxyphenyl)-3-heptanone	-9.1	-8.3	-8.7
4	Yakuchinone A	-8.5	-8.2	-8.5
5	3,5-dimethoxy-4- acetoxybenzyl alcohol	-6.9	-6.8	-6.6
6	<i>p</i> -Coumaric acid	-6.7	-6.8	-6.7
7	Clorgyline	-6.6	N.A	N.A
8	Nortriptyline	N.A	-9.9	N.A
9	Paroxetine	N.A	N.A	-10.2

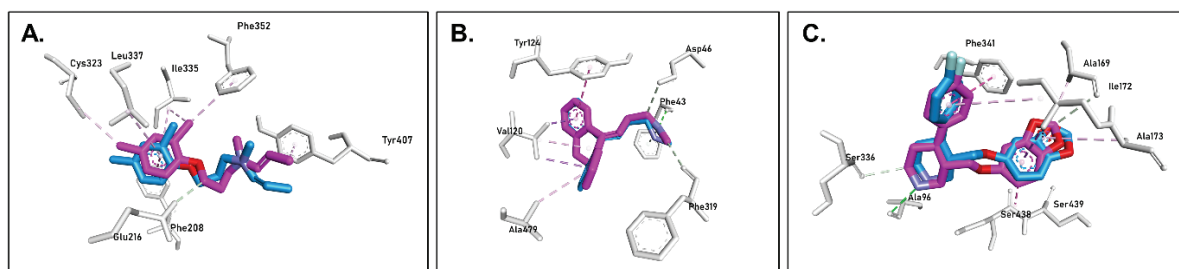


Figure 5. Visualization of the co-crystallized ligands (pink) overlapping with their redocked conformations (blue) in the respective binding sites. The RMSD values between the docked and crystallographic poses were (A) 1.220 Å for clorgyline on MAO, (B) 0.578 Å for nortriptyline on DAT, and (C) 0.723 Å for paroxetine on SERT. Green and pink dashed lines represent hydrogen bonds and hydrophobic interactions.

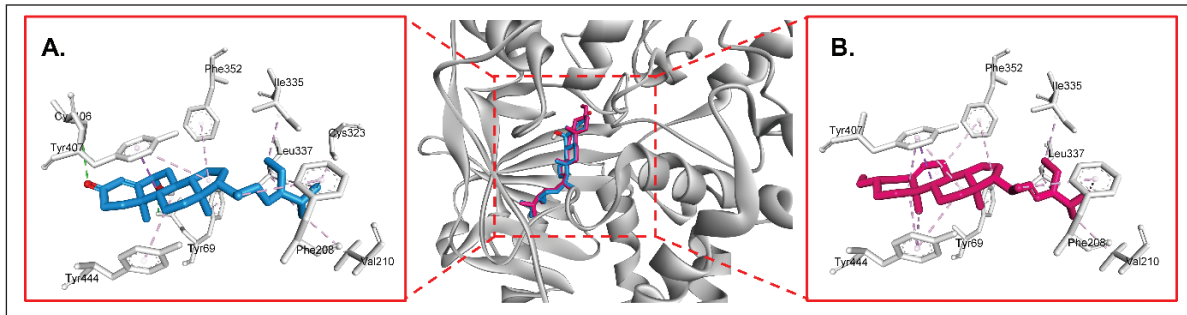


Figure 6. Molecular interactions of (A) stigmast-4-en-6 β -ol-3-one and (B) stigmasterol from *E. rubroloba* rhizome with MAO.

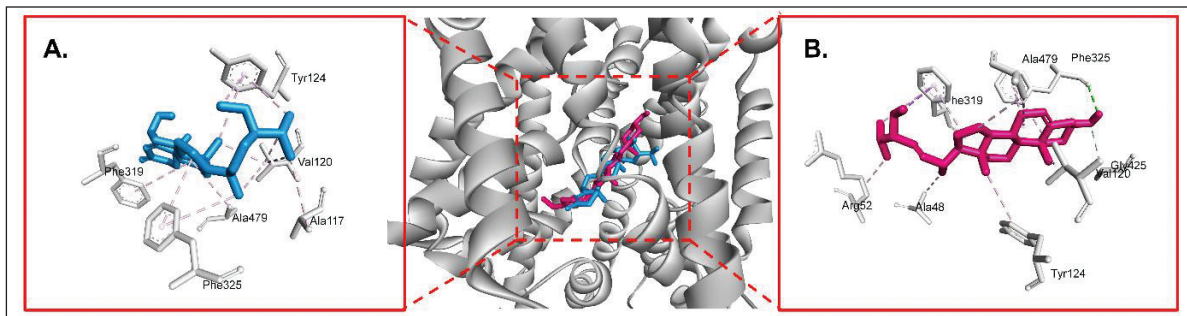


Figure 7. Molecular interactions of (A) stigmast-4-en-6 β -ol-3-one and (B) stigmasterol from *E. rubroloba* rhizome with DAT

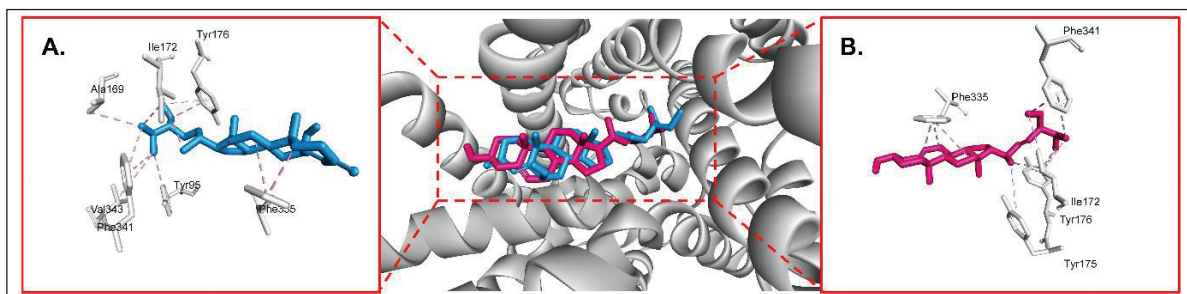


Figure 8. Molecular interactions of (A) stigmast-4-en-6 β -ol-3-one and (B) stigmasterol from *E. rubroloba* rhizome with SERT.

On the DAT, stigmast-4-en-6 β -ol-3-one and stigmasterol exhibited identical binding energies of -10.7 kcal/mol, which is lower than the control nortriptyline (-9.9 kcal/mol). Stigmast-4-en-6 β -ol-3-one interacts through strong hydrophobic interactions with key residues such as Val120, Ala117, Ala479, Tyr124, Phe325, and Phe319 (Fig. 7A) at the DAT binding site [30], indicating the compound's ability to effectively inhibit dopamine reuptake. Stigmasterol, on the other hand, forms hydrogen bonds with Phe325 and Gly425, potentially enhancing the stability of transporter inhibition. Additionally, it also forms hydrophobic interactions with residues Ala479, Phe319, Arg52, Tyr124, Ala48, and Val120 (Fig. 7B). In comparison, nortriptyline forms more hydrogen bonds (Phe43, Asp46, and Phe319) and hydrophobic interactions (Tyr124, Val120, and Ala479), but with a higher binding energy.

The DAT is responsible for the reuptake of dopamine from the synapse back into the presynaptic neuron after its release. Dopamine plays a key role in mood regulation, reward,

and motivation [31]. Inhibition of DAT can elevate dopamine levels in the synapse, potentially enhancing motivation and happiness—both aspects often disrupted in depressed patients [32]. Docking simulations revealed that stigmast-4-en-6 β -ol-3-one and stigmasterol have high affinities for DAT, with lower binding energies compared to nortriptyline (a tricyclic antidepressant). DAT inhibition by these compounds would increase dopamine levels in the brain, contributing to antidepressant effects. This aligns with the dopaminergic dysfunction theory of depression, which suggests that dopamine deficits contribute to symptoms of anhedonia and reduced motivation in depression.

On the SERT, stigmast-4-en-6 β -ol-3-one displayed a binding energy of -10.5 kcal/mol, which is lower than that of stigmasterol (-10.1 kcal/mol) and the control paroxetine (-10.2 kcal/mol). Stigmast-4-en-6 β -ol-3-one demonstrated strong hydrophobic interactions with residues Tyr176, Ala169, Phe341, Ile172, Val343, Tyr95, and Phe335 at the SERT

binding site (Fig. 8A) [22], similar to the inhibitory mechanism observed with DAT, indicating its potential to inhibit serotonin reuptake. Stigmasterol also showed good binding stability through interactions with similar residues as stigmast-4-en-6 β -ol-3-one (Fig. 8B). Although paroxetine exhibited slightly lower affinity, it formed hydrogen bonds with Ala96 and Ser336, providing additional stability to SERT inhibition. Overall, stigmast-4-en-6 β -ol-3-one appears to be superior to paroxetine in terms of binding energy, suggesting its potential as a stronger serotonin reuptake inhibitor with relevant clinical applications for increasing serotonin levels and alleviating depressive symptoms.

The SERT is a protein responsible for the reuptake of serotonin from the synaptic cleft back into the presynaptic neuron. Serotonin is a key neurotransmitter involved in mood regulation, anxiety, and well-being [33]. Selective serotonin reuptake inhibitors (SSRIs) function by blocking SERT, thereby increasing serotonin levels in the synapse and improving depression symptoms [34]. Molecular docking showed that stigmast-4-en-6 β -ol-3-one and stigmasterol have very low binding energies toward SERT, comparable to or even lower than paroxetine, an SSRI. Inhibition of SERT by these compounds may elevate serotonin concentrations in the synapse, contributing to mood improvement and the reduction of depression symptoms.

4. CONCLUSION

Firstly, six of the 48 major compounds of *E. rubroloba* rhizome have been isolated and identified: Stigmasterol (ER1), Stigmast-4-en-6 β -ol-3-one (ER2), Yakuchinone A (ER3), 1-(3'-methoxy-4'-hydroxyphenyl)-7-(4''-hydroxyphenyl)-3-heptanone (ER4), 3,5-dimethoxy-4-acetoxy cinnamyl alcohol (ER5), and p-Coumaric acid (ER6). ER3 and ER4 demonstrate strong antioxidant potential, while ER1 and ER2 exhibit significant anti-inflammatory properties. Computational analysis suggested that ER1 and ER2 have potential interactions with MAO, DAT, and SERT, which may be relevant to neurotransmission pathways involved in depression. These findings indicate a possible role of ER1 and ER2 in influencing dopamine and serotonin systems, warranting further *in vitro* validation.

5. ACKNOWLEDGMENT

We would like to thank to The Ministry of Education, Culture, Research, and Technology of the Republic of Indonesia for a research grant under scheme "KATALIS" Research 2024, with contract No. 151/UN29.20/PG/2024.

6. AUTHOR CONTRIBUTIONS

All authors made substantial contributions to conception and design, acquisition of data, or analysis and interpretation of data; took part in drafting the article or revising it critically for important intellectual content; agreed to submit to the current journal; gave final approval of the version to be published; and agree to be accountable for all aspects of the work. All the authors are eligible to be an author as per the International Committee of Medical Journal Editors (ICMJE) requirements/guidelines.

7. CONFLICTS OF INTEREST

The authors report no financial or any other conflicts of interest in this work.

8. ETHICAL APPROVALS

This study does not involve experiments on animals or human subjects.

9. DATA AVAILABILITY

All data generated and analyzed are included in this research article.

10. PUBLISHER'S NOTE

All claims expressed in this article are solely those of the authors and do not necessarily represent those of the publisher, the editors and the reviewers. This journal remains neutral with regard to jurisdictional claims in published institutional affiliation.

11. USE OF ARTIFICIAL INTELLIGENCE (AI)-ASSISTED TECHNOLOGY

The authors declare that they have not used artificial intelligence (AI)-tools for writing and editing of the manuscript, and no images were manipulated using AI.

REFERENCES

- Sahidin I, Wahyuni W, Hajrul MM, Jabbar A, Imran I, Manggau Marianti A. Evaluation of antiradical scavenger activity of extract and compounds from *Etilingera calophrys* Stems. *Asian J Pharm Clin Res.* 2018;11(2):238–41. doi: <https://doi.org/10.22159/ajpcr.2018.v11i2.22535>
- Fristiohady A, Leorita M, Malik F, Thamrin ASW, Ilyas MY, Wahyuni, *et al.* Pancreatic histological profile on the efficacy of extract of *Etilingera calophrys* (K. Schum) A.D. poulsen stem against streptozotocin-induced diabetes in diabetic model rats. *Biointerface Res Appl Chem.* 2021;11(2):9209–17. doi: <https://doi.org/10.33263/BRIAC112.92099217>
- Wahyuni SI, Rahim AR, Arba M, Yodha AMW, Nur Syifa Rahmatika NS, Rahmatika NS, *et al.* Radical scavenger and antimicrobe of diarylheptanoids and steroids from *Etilingera calophrys* rhizome. *Sustain Chem Pharm.* 2022;29(4):100767. doi: <https://doi.org/10.1016/j.scp.2022.100767>
- Wahyuni, Grashella SHL, Fitriah WOI, Malaka MH, Fristiohady A, Imran, *et al.* Antibacterial and antioxidant potentials of methanol extract and secondary metabolites from *Wualae* rhizome (*Etilingera elatior*). *CRBB.* 2019;1(1):13–6. doi: <https://doi.org/10.5614/crbb.2019.1.1/IHHZ547>
- Fristiohady F, Wahyuni, Ilyas MY, Bafadala M, Purnama LOMJ, Sangadji, *et al.* Nephroprotective effect of extract *Etilingera elatior* (Jack) R.M. Smith on CCl₄-induced nephrotoxicity in rats. *CRBB.* 2020;1(2):62–5.
- Fristiohady A, Sadarun B, Wahyuni Ilyas M, Malik F Purnama LOMJ, Bafadal M, Leorita M, *et al.* Hepatoprotective activity *Etilingera elatior* (Jack) R.M. Smith extract against CCl₄-induced hepatic toxicity in Male Wistar rats. *RJPT.* 2020;13(10):807. doi: <https://doi.org/10.5958/0974-360X.2020.00807.0>
- Imran, Wahyuni, Fristiohady A, Leorita M, Malaka MH, Ilyas MY, *et al.* Radical Scavenger and antidiabetic potencies of *Etilingera elatior* fruits growing in South East Sulawesi-Indonesia. *RJPT.* 2022;15(5):2141–6. doi: <https://doi.org/10.52711/0974-360X.2022.00355>
- Hamsidi R, Wahyuni W, Sahidin I, Apriyani E, Harsono H, Azizah NA, *et al.* Suppression of proinflammatory cytokines by *Etilingera*

- alba* (A.D.) poulsen rhizome extract and its antibacterial properties. *Adv Pharmacol Pharm Sci.* 2021;2021:5570073. doi: <https://doi.org/10.1155/2021/5570073>
9. Wahyuni, Diantini A, Ghozali M, Subarnas A, Julaeha E, Amalia R, *et al.* Phytochemical screening, toxicity activity and antioxidant capacity of ethanolic extract of *Etilingera alba* Rhizome. *PJBS.* 2021;24(7):807–14. doi: <https://doi.org/10.3923/pjbs.2021.807.814>
 10. Wahyuni, Diantini A, Ghozali M, Subarnas A, Julaeha E, Amalia R, Sahidin I. Cytotoxic and antimigration activity of *Etilingera alba* (A.D.) Poulsen rhizome. *Adv Pharmacol Pharm Sci.* 2021;2021:6597402. doi: <https://doi.org/10.1155/2021/6597402>
 11. Wahyuni, Diantini A, Ghozali M, Subarnas A, Julaeha E, Amalia R, *et al.* *In vitro* anticancer activity of chemical constituents from *Etilingera alba* (AD) poulsen against triple negative breast cancer and *in silico* approaches towards MMP-1 inhibition. *IJoST.* 2022;7(2):251–78. doi: <https://doi.org/10.17509/ijost.v7i2.50547>
 12. Ilyas MY, Diantini D, Halimah E, Amalia R, Ghozali M, Julaeha E, *et al.* Potential immunomodulator fraction fruits of *Etilingera rubroloba* A.D poulsen against macrophage phagocytosis and interleukin-12 levels in BCG-stimulated Balb/C Mice. *Int J Pharm Res.* 2021;13(1):3262–9. doi: <https://doi.org/10.31838/ijpr/2021.13.01.478>
 13. Ilyas MY, Diantini A, Ghozali M, Sahidin I, Fristiohady A. Immunomodulatory potency *Etilingera rubroloba* AD poulsen fruit ethanol extract against macrophage phagocytic activity and CD4 levels in wistar male rats. *RJPT.* 2022;15(9):4067–72. doi: <https://doi.org/10.52711/0974-360X.2022.00682>
 14. Jabbar A, Sahidin I, Malik F, Ilyas MY, Rusli N, Reymon, *et al.* Evaluation of xanthine oxidase inhibitory activity of sinapyl alcohol diacetate and stigmasterol compounds and phytochemical screening stem of *Etilingera rubroloba* A.D Poulsen. *Food Res.* 2023;7(4):101–5. doi: <https://doi.org/10.26656/fr.2017.7>
 15. Jabbar A, Ilyas M, Wahyuni, Hamzah H, Windarsih A, Pratiwi SUT, *et al.* LC-MS Analysis, antioxidant and anti-inflammatory activities, isolation of secondary metabolite of ethanol extract stem of *etilingera rubroloba* AD Poulsen. *CSCEE.* 2024;10:100780. doi: <https://doi.org/10.1016/j.cscee.2024.100780>
 16. Sanghvi K, Chandrasheker KS, Pai V. Review on *Curcuma longa*: ethnomedicinal uses, pharmacological activity and phytochemical constituents. *RJPT.* 2020;13(8):3983–6. doi: <https://doi.org/10.5958/0974-360X.2020.00704.0>
 17. Singh D, Upadhyay P. Antiinflammatory and wound healing activity of curcumin containing phytosomes, niosomes and liposomes in rats. *RJPT.* 2023;16(6):2776–8. doi: <https://doi.org/10.52711/0974-360X.2023.00456>
 18. Souza AL, Patti GJ. A protocol for untargeted metabolomic analysis: from sample preparation to data processing. *Methods Mol Biol.* 2021;2276:357–82. doi: https://doi.org/10.1007/978-1-0716-1266-8_27
 19. Hamsidi R, Adianti M, Septriana M, Priskila O, Fristiohady A, Malaka MH, *et al.* Characteristic of the ethanol extract of *Carthamus tinctorius* L. flowers and its antioxidant activity. *RJPT.* 2023;16(2):791–8. doi: <https://doi.org/10.52711/0974-360X.2023.00136>
 20. Zomba D, Dar MA, Singh R, Batish DR, Kaur S. Exploring the antimicrobial, antioxidant, and *in vitro* anti-inflammatory potential of *Oxytropis microphylla* (Pall.) DC. plant species of Ladakh region. *Discov Food.* 2025;5:246. doi: <https://doi.org/10.1007/s44187-025-00553-w>
 21. De Colibus L, Li M, Binda C, Lustig A, Edmondson DE, Mattevi A. Three-dimensional structure of human monoamine oxidase A (MAO): relation to the structures of rat MAO A and human MAO B. *PNAS USA.* 2005;102(36):12684–9. doi: <https://doi.org/10.1073/pnas.0505975102>
 22. Coleman JA, Green EM, Gouaux E. X-ray structures and mechanism of the human serotonin transporter. *Nature.* 2016;532(7599):334–9. doi: <https://doi.org/10.1038/nature17629>
 23. Morris GM, Huey R, Lindstrom W, Sanner MF, Belew RK, Goodsell DS, *et al.* AutoDock4 and AutoDockTools4: automated docking with selective receptor flexibility. *J Comput Chem.* 2009;30(16):2785–91. doi: <https://doi.org/10.1002/jcc.21256>
 24. Arfan A, Asnawi A, Aman LO. Marine sponge *Xestospongia* sp.: a promising source for tuberculosis drug development-computational insights into mycobactin biosynthesis inhibition. *Borneo J Pharm.* 2024;7(1):40–50. doi: <https://doi.org/10.33084/bjop.v7i1.5513>
 25. Trott O, Olson AJ. AutoDock Vina: improving the speed and accuracy of docking with a new scoring function, efficient optimization, and multithreading. *J Comput Chem.* 2010;31(2):455–61. doi: <https://doi.org/10.1002/jcc.21334>
 26. Sahidin I, Malaka MH, Fristiohady A, Saleh A, Marianti A.. Antibacterial and radical scavenger activities of extract and compounds of Wualae (*Etilingera elatior*) stems from Southeast Sulawesi. *IOP Conf Ser Mater Sci Eng.* 2019;546(6):62027. doi: <https://doi.org/10.1088/1757-899X/546/6/062027>
 27. Della Greca M, Monaco P, Previtera L. Stigmasterols from *Typha latifolia*. *J Nat Prod.* 1990;53(6):1430–5. doi: <https://doi.org/10.1021/np50072a005>
 28. Fristiohady A, Malaka MH, Safitri ARW, Diha D, Purnama LOMJ, Rahman S, *et al.* Anti-inflammatory activity of ethanol extract of marine sponge *Petrosia* Sp. by suppression the level of tumor necrosis factor-alpha. *RJPT.* 2021;14(8):4435–9. doi: <https://doi.org/10.52711/0974-360X.2021.00770>
 29. Wang CC, Billett E, Borchert A, Kuhn H, Ufer C. Monoamine oxidases in development. *CMLS.* 2013;70(4):599–630. doi: <https://doi.org/10.1007/s00018-012-1065-7>
 30. Penmatsa A, Wang KH, Gouaux E. X-ray structure of dopamine transporter elucidates antidepressant mechanism. *Nature.* 2013;503(7474):85–90. doi: <https://doi.org/10.1038/nature12533>
 31. Soni S, Verma L. Nicotine and neurotransmitters an update. *RJPT.* 2024;17(6):2605–12. doi: <https://doi.org/10.52711/0974-360X.2024.00407>
 32. Belujon P, Grace AA. Dopamine system dysregulation in major depressive disorders. *Int J Neuropsychopharmacol.* 2017;20(12):1036–46. doi: <https://doi.org/10.1093/ijnp/pyx056>
 33. Bremshey S, Groß J, Renken K, Masseck OA.. The role of serotonin in depression—A historical roundup and future directions. *J Neurochem.* 2024;168:1751–9. doi: <https://doi.org/10.1111/jnc.16097>
 34. Arias HR, Targowska-Duda KM, García-Colunga J, Ortells MO. Is the antidepressant activity of selective serotonin reuptake inhibitors mediated by nicotinic acetylcholine receptors?. *Molecules.* 2021;26(8):2149. doi: <https://doi.org/10.3390/molecules26082149>

How to cite this article:

Sahidin S, Fristiohady A, Muzuni M, Ahmad SW, Yodha AWM, Arfan A, Rahman DA, Wahyuni W, Batubara I, Kuspradini H, Earnestly F, Sundowo A. Secondary metabolites from *Etilingera rubroloba* rhizome: Profiling, isolation, structural elucidation, and evaluation of biological activities. *J Appl Pharm Sci.* 2026;16(04):233-244. DOI: 10.7324/JAPS.2026.273356